

RIGA TECHNICAL UNIVERSITY
Faculty of Electrical and Power Engineering
Institute of Industrial Electronics and Electrotechnic

Roman Graf

Doctorand of the doctorate programme "Electroactuator and Automation"
(student paper number 921E1304O)

**MICROACTUATOR DEVICE FOR TACTILE-GRAPHICAL
TRANSMISSION TO VISUALLY IMPAIRED PEOPLE**

Dissertation

Scientific head
Dr. Habil. Sc. Eng., professor
JANIS GREIVULIS

RTU Publishing House
Riga - 2004

**DISSERTATION
FOR THE DOCTOR DEGREE OF ENGINEERING SCIENCES
RIGA TECHNICAL UNIVERSITY**

Dissertation to receive a doctorate of engineering sciences will be publicly defended
..... 2004 in..... Faculty of Electrical and Power Engineering
at Riga Technical University with the address

DISSERTATION COMMITTEE

Professor, Dr. Habil. Eng. Sc. J. Raņķis,
Riga Technical-University, Latvia

Professor, Dr. Habil. Eng. Sc. J. Osis,
Riga Technical University, Latvia

Professor. Dr. Habil. Eng. Sc. A. Šnīders,
Latvian Agriculture University, Latvia

CONFIRMATION

I confirm, that I have developed this dissertation, hereby presented for the examination at Riga Technical University, to acquire a doctor degree of engineering sciences. The dissertation is not presented at any other university for such a purpose.

Roman Graf

Date:

The dissertation is written in Russian language, contains the annotation, the list of symbols, 4 chapters, the conclusion, the links to 44 bibliographical sources, 5 appendixes, 37 pictures and diagrams. It is written on 103 pages.

CONTENTS

Contents	4
List of symbols	5
General work description	8
Actuality of work	8
The purpose, object and tasks of research	8
Research methods and scientific novelty of work	8
Obtained results and practice use of work	9
Work aprobation	9
Patent of invention	10
Structure and short annotation of work	10
1. Object of research and task definition	11
1. Microactuator analysis of the tactile-graphical pattern module for visually impaired persons	12
3. Braille display control system	20
3. Natural tactile-graphical module sample and logical algorithms of its work	27
General conclusion	34
References	35
Autor publications	35
Patent of invention	35

LIST OF SYMBOLS

I chapter:

SMA - shape memory alloys.

II chapter:

Ni-Ti	- alloy from nickel and titan;	
S	- wire diameter;	[cm ²]
A _s	- lower bound of the austenite temperature;	[°C]
A _F	- tipper bound of the austenite temperature;	[°C]
M _s	- lower bound of the martensite temperature;	[°C]
M _F	- upper bound of the martensite temperature;	[°C]
γ	- shearing of Ni-Ti lattice;	[m]
τ	- shear load;	[N]
Φ	- potential energy of the SMA layers;	[J]
Φ ₀	- potential energy of the SMA layers without load;	[J]
t	- time of heating or cooling of the SMA wire;	[s]
F _s	- static force;	[N]
F _{din}	- dynamic force;	[N]
P ₀	- load;	[N]
J	- Joule energy;	[J]
K _F	- coefficient;	
K _{A,M}	- coefficients far the austenite and the martensite phases;	[1/J]
L	- length of the SMA wire;	[m]
R	- resistance of the SMA wire;	[Ω]
W _e	- consumed power for the one SMA wire;	[W]
I	- current through the SMA wire;	[A]
U	- voltage on the SMA wire;	[V]
V _L	- velocity of the raicroactuator length changes;	[m/s]
t ₀ , t ₁ , t ₂	- calculation points for the time in the mathematical model;	[s]
L ₀ , L ₁ , L ₂	- calculation points for the length in the mathematical model;	[m]
a, b, c, m, n	- coefficients for the mathematical model calculation;	
x, y, z	- co-ordinate ass;	
T	- temperature of Ni-Ti wire;	[°C]
α	- thermal expansion;	[1/°C]
β	- thermal conductivity;	[W/cm°C]
ρ	- specific resistance;	[Ωcm]
ρ ₀	- normal specific resistance;	[Ωcm]
κ	- thermal transmission coefficient;	[W/cm ² °C]
κ ₀	- surface effect coefficient;	
ϑ	- temperature of the wire under a current;	[°C]
ϑ ₀	- normal temperature;	[°C]
ϑ _n	- lower bound of the temperature;	[°C]
ϑ _γ	- stabilized temperature;	[°C]
C	- heating temperature constant;	[°C]
δ	- current density;	[A/cm ²]

m	- density;	[g/cm ³]
c	- thermal capacity coefficient;	[J/cm ³ °C]
c _o	- normal thermal capacity;	[J/cm ^{3a} C]
τ	- substitution constant.	

III chapter:

DCCCM	- directactuated collectorless constant current motor;
RPS	- rotor position sensor;
ARS	- automatically regulation system;
I ² C	- Internal Integrated Circuit - standard for the successive date transmission;
N _K	- digital code" of the given Braille display carriage position;
N _d	- motor control signal code;
MOTOR FG	- motor rotation frequency sensor signal;
N _F	- absolute position sensor signal of the Braille display carriage;
MOTOR CTL	- outgoing signal of the servocontroller;
MOTOR REV	- motor reverse signal;
CURRENT	- stator current overloading signal;
LIMIT	
N _c	- motor rotation velocity code;
PG	- rotor position sensor signal;
PK	- Braille display carriage relative position signal;
p	- Laplace operator;
X _F	- real carriage position;
X _K	- carriage position given by code N _K ;
X _{FS}	- real carriage position with the transmission function calculation of the carriage position sensor;
ΔX	- difference between X _K and X _{FS} ;
K _o	- proportionality coefficient;
K _N	- nonlinearity coefficient as a function from (X _F -X _K);
T ₁	- time constant of the transition process;
W _{MP}	- transmission function of the servocontroller and the motor;
W _{S(p)}	- transmission function of the carriage position sensor;
W _{SI(p)}	- transmission function of the delay gain;
W _{SD(p)}	- transmission function of the inertial gain;
WE(P)	- transmission function of the opened system;
Wz(p)	- transmission function of the closed system;
K ₁	- transmission coefficient of the servocontroller and the motor;
T _{S1} , T _{S2}	- time constants;
H(t)	- normalised transmission characteristic.

IV chapter:

λX	- intensity of the crashes;	[1/h]
t	- time interval;	[h]
Q	- probability of the crashes;	[h]
T_{el}	- average work time before the crash for a display element;	[h]
T_m	- average work time before the crash for the whole module;	[h]
P(t)	- crashless work probability during the 20 years period;	[%]
T_o	- one cycle of the microactuator work;	[s]
T_H	- subcycle of the information storage (reading);	[s]
T_R	- subcycle of the information record in a matrix;	[s]
T_E	- subcycle of the information erasure;	[s]
T_S	- time constant of the tactile feelings;	[s]
l	- quantity of the RAM address ranking;	
n	- quantity of the SMA wires;	
U	- direct voltage;	[V]
Si	- electrical switches for each of the module taxels;	
W	- electrical power for the whole module;	[W]
I	- electrical current for each element.	[A]

GENERAL WORK DESCRIPTION

Actuality of work

One of the prior directions of the scientific research and the development of technologies is the creation of a wide range of technical devices, which allow visually impaired people to fully take part in the society. The eyesight is most important human channel for receiving information. More than two thirds of its full volume is received as visual pictures. The ability of visually impaired people (partly or fully blind) to receive information, consequently to develop the professional skill, is therefore substantially diminished. Modern technology and society life are tightly bounded with computer technologies and the ability to use a computer can be seen as one of the indications of technical and social progress. Therefore, the task of developing of an economically and technically effective interface (people-computer) device has become an actuality. Such a device has to support the communication between visually impaired people and personal computers.

According to the functionality principle such a device has to be tactile - graphical. It has to transform the visual information in its tactile equivalent. Since the idea of such a transformation belongs to Braille, who created a special convexity script, a logical name for this interface module could be "tactile - graphical Braille display". As part of this work an analysis of existing tactile devices has been made. The analysis shows, that such a device, mostly constructed to transmit a Braille text and a graphical presentation, does not exist. The principal scientific-technical problem in the development of a tactile-graphical display is the creation of a system of microactuators which are able to support relief patterns on a relative big square by giving dynamical qualities.

Purpose, object and tasks of research

The purpose of this dissertation is the development of qualitative tactile - graphical Braille display. The display should be able to quickly present a tactile - graphical picture with a high resolution and a high reliability. It should also need a relatively low manufacturing costs.

To achieve this purpose, it was necessary to make theoretical and experimental research in the following directions:

- development of technical demands for a tactile-graphical Braille display, based on psycho - physiological qualities of the user analysis;
- research of different methods to form a dynamical relief patterns;
- theoretical and experimental research of structures and schematic - technical solutions, which can realise chosen principle to form dynamical relief patterns;
- analysis of dynamical properties of a motor - controlled system, as a key element of this tactile - graphical display;
- development of electrical schemas;
- construction of principal functional nodes of a tactile-graphical Braille display.

Research methods and scientific contribution

The research and the development in accordance to the goal has been made by methods of mathematical, computer and physical modelling. For experiments have been used the technical base and the labour equipment of The Institute for Micro Technique and Precision Engineering at The Vienna University of Technology, measuring system was

DEWETRON, and the software products were DasyLab 4.01.10 and Microsoft Excel 2000. The scientific novelty of this dissertation consists of:

- the development of technical prerequisites for a tactile - graphical Braille display, based on psycho -physiological qualities of a user analysis;
- the method to form dynamical relief patterns in a tactile - graphical Braille display, based on SMA (shape memory alloys) wires matrix;
- the analysis of the behaviour of SMA wires in display structures;
- the analysis of the thermal (heating/cooling) behaviour of SMA wires in display structures;
- the development of the structure of a movable tactile-graphical Braille display module and the structure of its control node;
- the analysis of dynamical properties of the motor - control system of the display;
- the method to generate a relief pattern based on the cycle approach to SMA wires control.

The scientific novelty of this construction of a tactile-graphical Braille display has been approved by the patent of invention.

Results and applications

The obtained results allow to resolve the task of the creation of a qualitative tactile - graphical Braille display. Six papers have been published including information about this research. With a support of the technical base and the labour equipment of The Institute for Micro Technique and Precision Engineering at The Vienna University of Technology, a sample of movable Braille display tactile module has been build and tested. Developed construction allows better integrate visually impaired people in society and elongate their education and work possibilities.

Approbation of results

The approbation of research results' of the author has been made by taking part in scientific-technical conferences:

- Micro Actuation Principles for Tactile Graphic Displays (state of the art and recent efforts). Proc of the MME99, September 27-28, 1999, Gif sur Yvette, France, pp. 247-250.
- Development of micro - actuators for tactile graphic displays (state of the art and recent efforts). Proc of the 22nd International Conference on Microelectronics (MIEL 2000), Vol 2, may 14-17, 2000, Nis, Serbia, pp. 573-576.
- Šķidrumu ar īpašajām elektriskajām strukturām pielietojums Braila displeja izveidē, "Enerģētika un elektrotehnika" RTU zinātniskie raksti, serija 4, sejmums 5, Rīga 2002, izdevniecība RTU, lpp. 110-113.
- Braila displeja dzinēja vadības sistēmas dinamisko raksturlīkņu analīze, "Enerģētika un elektrotehnika" RTU zinātniskie raksti, serija 4, sejmums 7, Rīga 2002, izdevniecība RTU, lpp-105-110.
- Experimental Research: Shape Memory Alloys - Actuator for Using in Movable Graphical Device for Visually Impaired People, Mikroelektronik 2003, October 1-2, 2003, Vienna, Austria.

Patent of the invention

The scientific novelty of the construction of functional nodes of a tactile-graphical Braille display has been approved by the Austrian patent of invention: A 259/2003, "Kompaktes Bewegliches Taktiles Modul Mit Formgedachtnislegierungen-Antrieb", 20.02.2003.

Structure and short annotation of work

This work consists of: a microactuator for tactile-graphical patterns, an experimental system to investigate microactuator characteristics, a graph-analytical method of an analytical research of the microactuator, a control system for Ni-Ti-microactuator and a natural tactile-graphical display model.

In the first chapter is presented the actual state of art. The examination has been done through the patent and bibliographical research. In particular were analysed the existing concepts of a Braille display construction method. The advantages and disadvantages of patented devices and manufacture costs are described. The task of the dissertation is explained from the medical point of view. In this chapter are described problems of visual impaired people. The prerequisites for a Braille display construction, which are conform with Braille type geometry, are considered. A concrete concept and a principle solution for a Braille display construction is presented.

In the second chapter is described the construction and the usage of the experimental system to investigate an Ni-Ti-microactuator. His static and dynamic characteristics are analysed. Graph-analytical calculation results are compared with experimental data. A calculation of the spent energy has been made. The research results are compared to the task of a microactuator. His usability for a Braille display construction has been investigated.

In the third chapter is the research of the control principles. A control system to control microactuators and motors has been defined. A type of motor has been chosen to control a tactile-graphical module. The structure of an automatically controlled system has been found out. The efficiency of this control method, based on the two-channel ARS, has been confirmed by the results of the analysis of dynamical characteristics.

In the fourth chapter is presented the usage of the developed construction. In this part are described natural movable Braille display modules, A method of its manufacturing and using has been considered, hi this part is given a new alternative solution of the problem and its argumentation. Based on the experimental research of microactuator features, a sample of a movable Braille display module has been build. Its advantages and disadvantages were compared.

1. OBJECT OF RESEARCH AND TASK DEFINITION

In the first chapter are developed the demands for the Braille display construction. Braille display is a device, which allows visually impaired persons to scan from a display generated tactile pattern by moving the finger upon it. On the display surface is placed a plurality of independently controllable movable actuator elements (pattern points). They are placed in a raised or in a drooped position. Their ordered positions present tactile-graphical picture or text.

Table 1.1.

Classified demands to Braille display construction

Demands	Minimum	Wished	Ideal	Measurement values	Explanation
Distance between taxels	0.8	1.5	<1.00	mm	Braille geometry
Taxel diameter	0.6	0.6-1	0.8	mm	Braille geometry
Taxel height	0.4	0.6-1.2	0.8-1	mm	Braille geometry
Quantity of taxels	6930	27580	>62370	taxels	square of device
Distance between letters	3.0	3.5	3.5	mm	Braille geometry
Distance between rows	4.0	5.0	5.0	mm	Braille geometry
Load on taxel	0.02	<0.3	0.05-0.15	N	microactuator properties
Time of one cycle	>10	<1	0.1-1	s	control technique
Square of device	26x20	297x210	640x480	mm	using in office
Braille display costs	1000	<1000	<500	Ls	manufacture costs

Demands for tactile pattern geometry developed in table 1.1: the distance between taxels has to be 1mm, taxel diameter 0.8mm, taxel height 1mm. Together about 27580 taxels. Load on a taxel 0.05N. Square of the device 297mm x 210mm. Time of one pattern setting cycle 1 second. Assumption costs of device 500Ls – 1000Ls.

Mechanical, piezoelectric and electromagnetic microactuators do not allow the creation of a pattern with high resolutions and have a complex construction. Mechanical and electromechanical microactuators have a low reliability. Known constructions of the electrostatic microactuator can not exert needed opposite forces to the user's finger. Microactuator from a special polymer is not in accordance to the demand of the tactile pattern setting time. Electro - rheological microactuator has a complex construction and operate with a high voltage, what reduces the construction reliability.

From the patent and the literature research about tactile-graphical devices for visually impaired people [8, 11] has been concluded that reliable, economical and constructional argued construction does not exist at the moment. Presented devices are mostly constructed to present a Braille text. A graphical pattern presentation was not included. Single devices for the graphic presentation were constructed, but they only partly match to demands of graphical patterns for visually impaired persons.

2. MICROACTUATOR ANALYSIS OF THE TACTILE- GRAPHIC AL PATTERN MODULE FOR VISUALLY IMPAIRED PERSONS

The second chapter is dedicated to the microactuator for a tactile-graphical Braille display. The combination of in the first chapter described demands, defines a choice of wires as executive elements made from Ni-Ti alloy for the information module (microactuator). These materials belong to so called shape memory alloys [8, 9]. The main reason for the use of Ni-Ti alloys is its strong electrical resistance. It can be directly activated by applying the current. The shape effect is based on the phase transition in crystalline lattice of alloy. This effect is called in literature martensitic transformation [4]. During this process in the lattice occur non - diffusion transformations between different kinds of the so called martensite phase or from the martensite phase in austenite. Depending on their shearing γ , the parts of lattice have the potential energy depicted on the figure 2.1.

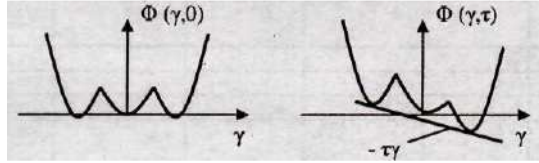


Fig.2.1. Potential energy of a lattice particle as a function of its shearing

Three potential convex parabolas correspond to the phases mentioned above. Under the load of shear τ , a work $-\tau\gamma$ is produced, which has to be added to the potential energy as it is shown in figure 2.1 (right).

$$\Phi(\gamma) = \begin{cases} \frac{1}{2} K_M (\tau\gamma - J)^2 & , \\ \frac{1}{2} K_A (\tau\gamma)^2 + \Phi_0 & , \\ \frac{1}{2} K_M (\tau\gamma + J)^2 & . \end{cases} \quad (2.1)$$

Equilibrium (2.1) describes a dependence of the static force F_{st} of a SMA wire from the dynamical force F_{din} . With the load P_0 , the static force F_{st} of a SMA microactuator is in its nature a reaction of prop $F_{st} = -P_0$. The dynamical force F_{din} can be found as:

$$F_{din} = \frac{d\Phi}{dL} k_F \quad (2.2)$$

where k_F - is a non size coefficient, (near to 1), including partly the transformation of the potential energy of an elementary SMA layer in the kinetic energy of the Browns motion. Therefore the additional exertion created by a wire is:

$$F_{st} + F_{din} = \frac{d\Phi}{dL} k_F - P_0. \quad (2.3)$$

By the direct control of the SMA wire, the electrical current causes the heating (Joule) energy J , and the change $\Delta\Phi$ of the potential energy of an SMA layers is:

$$\Delta\Phi \approx J \quad , \quad (2-4)$$

$$J = UI\Delta t \quad , \quad (2-5)$$

where I is the electrical current applied during the time interval Δt .

Going from final increases $\Delta\Phi$ to infinitesimal values $d\Phi$, and substituting the equation (2.5) in (2.3), we obtain the law of the microactuator control:

$$F_{st} + F_{dn} = \frac{U(t)I(t)}{V_L} k_F - P_0 \quad , \quad (2.6)$$

where

$$V_L = \frac{dL}{dt} \quad , \quad (2.7)$$

is the velocity of the change of the microactuator's length.

The presented experimental investigation of a microactuator [7] has an aim to find out the dependence of the length of an Ni-Ti wire from the time $L=f(t)$, as the next step to derive the velocity V_L of the Ni-Ti wire contraction from equations (2.6) and (2.7). One of the used variants in the experiment is the Ni-Ti wire [11] of diameter 50(μ m), work temperature 90°C, maximal load 0,343N, resistance 4,72 Ω by 10mm length (it depends on the length of wire), and the minimal current 50mA. The recommended load for this wire is between 0,034N < F < 0.343N.

To achieve length changes of 1 mm, we assume that, by heating, the wire contracts its length for about 3%. Then minimal wire length L for experiment has to be $L=1\text{mm}/0,03\approx 30\text{mm}$. For this length the expected power is $W_e = I^2R = 0,07\text{W}$. Experiment was made for wires with lengths: 10mm, 20mm, 30mm, 40mm, 50mm and 60mm. For each of these cases the loads 0.049N, 0.147N and 0.245N were applied.

The measuring method of SMA-alloy's properties is based on the laser light reception by a photo element, as well as the intensity changes on it caused by SMA-wire movements depending on the electrical voltage applied to the wire [2].

The measurement results show that, by heating, the contraction of the wire occurs quicker under smaller loads as under bigger loads. It happens because (fig.2.2) the contraction force depends on the electrical resistance, length and the diameter of the wire, and finally on the electrical current. Therefore, wire contracts slower by bigger loads, because the overforcing of larger opposite forces needs more time. The longer the wire, the stronger is its electrical resistance, the higher is the wire temperatures, and consequently the faster are the wire contracts.

As it can be seen in fig.2.2.f, the wire with 10mm length can not achieve a necessary force for the 1mm change of length. Wire with 20mm length (fig.2.2.e) achieves this difference in 0,45 seconds by the load 0,049N. By the load 0.147N, this wire needs already about 1 second. And by the load 0,245N, it can not achieve the necessary change of length.

The wire of length 30mm (fig.2.2.d) achieves the necessary length difference with all of the loads. Especially fast method to achieve 1mm change of length is to use the wire of length 60mm (fig.2.2.a). By the load of 0,049N, the contraction takes only 0,1 seconds (see table 2.1).

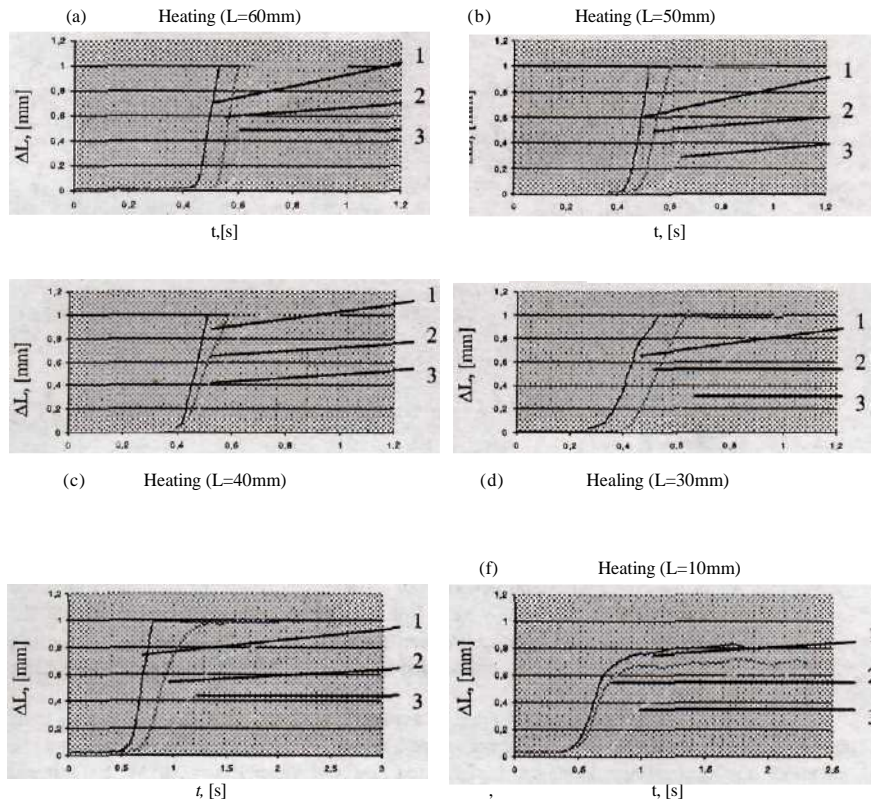


Fig.2.2. Characteristics showing the length changes during the test of heating a wire in dependence of its load: 1 corresponds to the load of 0.049N, 2 corresponds to the load of 4N and 3 corresponds to load 0.245N

The cooling of wire, as depicted in figure 2.3, causes its elongation. The longer the wire, the faster it elongates, because its surface is greater. Also, the stronger opposite force (in the experiment it is the weight, in a natural module it is the linear spring) applied to the wire, the faster it elongates.

Table 2.1.

The results of the experiment with SMA wire

Load, [N]	Length of the wire, [mm]	Resistance of the wire, [Ω]	Electrical power, [W]	Contraction time, [s]	Elongation time, [s]
0,049	20 - 40	9,4 - 18,8	0,046 - 0,092	0,12 - 0,30	0,12 - 0,25
0,147	20 - 40	9,4 - 18,8	0,046 - 0,092	0,18 - 0,60	0,09 - 0,24
0,245	30 - 40	14,1 - 18,8	0,069 - 0,092	0,30 - 0,70	0,05 - 0,23

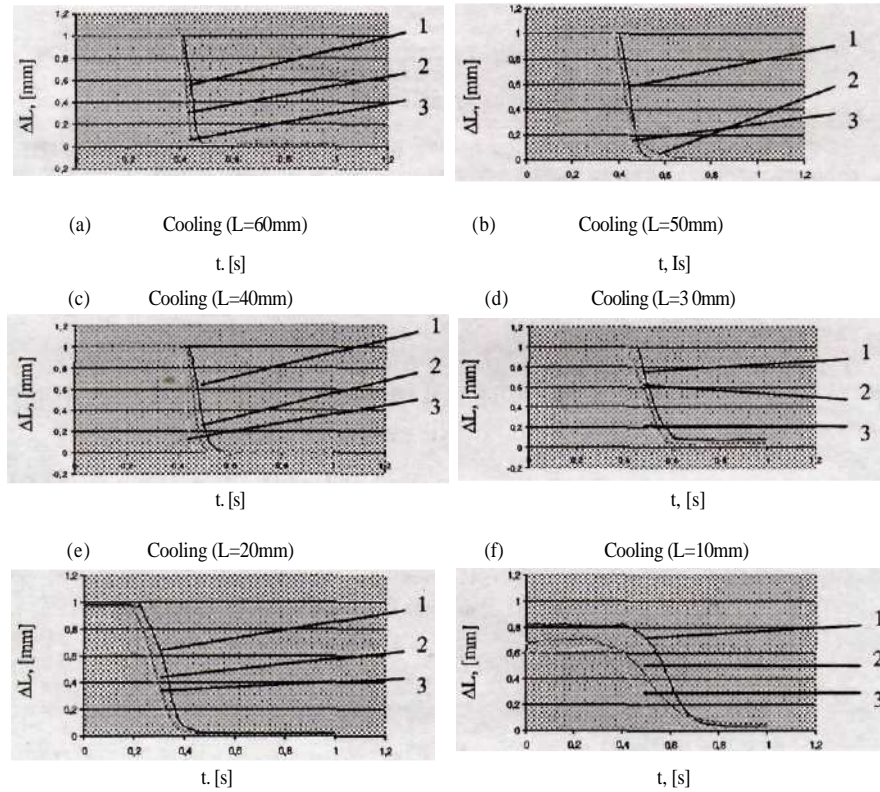


Fig.2.3. Characteristics showing the changes of length during the test of the cooling of wire in dependence of its load: 1 corresponds to load 0,049N, 2 corresponds to load 0,147N and 3 corresponds to load 0.245N

Wire made from shape memory alloys, with diameter 50nm and length 30mm produces enough force to work against opposite forces (fig.2.2.d). With the load 0,049N, it's contraction time is 0,15 seconds, with loads 0,147N - 0,4 seconds, and with loads 0.245N - 0,7 seconds. Also, wire elongates enough fast by cooling (fig.2.3.d). With the optimal load 0,049N, it's elongation time is 0,17 seconds.

Therefore Ni-Ti wire with this parameter is basically used as a microactuator for the tactile-graphical device for visually impaired persons.

For the mathematical modelling of a microactuator a wire of 30mm length has been chosen. As a load for this calculation, the optimal load 0,049N has been taken.

The dependence $L=f(t)$ can be generally calculated by a Lagrange polynomial for three calculation points:

$$L = \frac{(t-t_1)(t-t_2)}{(t_0-t_1)(t_0-t_2)} L_0 + \frac{(t-t_2)(t-t_0)}{(t_1-t_0)(t_1-t_2)} L_1 + \frac{(t-t_0)(t-t_1)}{(t_2-t_0)(t_2-t_1)} L_2 . \quad (2.8)$$

Taking into account the complex character of the function it is reasonable to divide it in two simpler functions.

$$L = \begin{cases} f_1(t) , & \text{in limits } T = 23^\circ\text{C till } T = 68^\circ\text{C;} \\ f_2(t) , & \text{in limits } T = 68^\circ\text{C till } T = 90^\circ\text{C.} \end{cases} \quad (2.9)$$

Function $f_1(t)$ characterises the heating process from the cool state, by a room temperature, till the austenite starting temperature A_s , when the shape memory effect begins. Function $f_2(t)$ characterises the heating process from the austenite starting temperature A_s , till the final austenite temperature A_f . After achieving the final austenite temperature, the shape memory effect leaves off. Using the appropriate mathematical transformation, the equation (2.9) becomes:

$$L = \begin{cases} 4,6t^2 - 0,26t + 0,012 & , \text{ in limits } [0;0] \text{ till } [0,24;0,21]; \\ 4,3t - 0,85 & , \text{ in limits } [0,243;0,2] \text{ till } [0,429;1]. \end{cases} \quad (2.10)$$

By cooling of a wire with the optimal load 0.049N (fig.2.3.d), the calculation of the function $L=f(t)$ is similar. Therefore, the equation (2.9) becomes:

$$L = \begin{cases} -8,14t + 0,97 & , \text{ in limits } [0;0,97] \text{ till } [0,4;0,07]; \\ 1,94t^2 - 0,71t + 0,06 & , \text{ in limits } [0,4;0,07] \text{ till } [0,21;0,08]. \end{cases} \quad (2.11)$$

The Joule energy for the equation (2.6) can be calculated graph-analytically from the equation

$$dW = [I(t)]^2 R(t) dt. \quad (2.12)$$

By the integration of this equation, to calculate the energy emission during a period of time t [6], it is necessary to consider the functions $I(t)$ and $R(t)$. The value $I(t)$ during the heating process may be taken as constant. The value $R(t)$ is the function of the wire temperature and depends on time. The resistance of the wire is defined by the formula

$$R = \frac{k_0 \rho L}{\delta} [\Omega] \quad (2.13)$$

The dependence of the wire electrical resistance from the temperature describes the formula:

$$\rho = \rho_0 (1 \pm \lambda \vartheta \pm \beta \vartheta^2 \pm \dots) \quad (2.14)$$

At normal temperatures of conductive metals ($<300^\circ\text{C}$) it is possible to limit the calculation to the first two members of this row:

$$\begin{aligned} dW &= I^2 \frac{k_0 L}{\delta} \rho_0 (1 + \alpha(90 - 67e^{-4,92t}) + \beta(90 - 67e^{-4,92t})^2) dt = \\ &= I^2 \frac{k_0 L}{\delta} \rho_0 (1 + \alpha 90 - \alpha 67e^{-4,92t} + \beta 8100 - \beta 180 \times 67e^{-4,92t} + \beta \times 67^2 e^{-9,84t}) dt. \end{aligned} \quad (2.15)$$

To calculate the velocity VL of Ni-Ti wire length changes from the equation (2.7), the graph-analytical calculation method for the function $L=f(t)$ can be used. For the calculation of the Ni-Ti current conductive wire heating transformation processes [6], some simplifications are made. A homogeneous current conductive system, where current density in all points of the wire is the same during the heating process by current heating, we can assume as a solid body with endless big heat conductivity, because there are no temperature differences.

Therefore:

$$\frac{d\vartheta}{dx} = \frac{d\vartheta}{dy} = \frac{d\vartheta}{dz} = 0. \quad (2.16)$$

Without external heat sources, heating equation is

$$c_0(1 + \beta\vartheta)m \frac{d\vartheta}{dt} = \delta^2 \rho_0(1 + \alpha\vartheta) - \frac{kL}{S}(\vartheta - \vartheta_0) \quad (2.17)$$

Temperature dependence of heat capacity for conductive materials is small and we may assume it is constant. The equation (2.17) becomes:

$$cm \frac{d\vartheta}{dt} = \delta^2 \rho_0(1 + \alpha\vartheta) - \frac{kL}{S}(\vartheta - \vartheta_0) \quad (2.18)$$

We assume the same diameter along the whole length of the wire, and the same value and the character of current density changes at each moment of time, therefore we assume the case of a heating system which is similar to the linear current conductive system. These conditions correspond to the equation (2.18), which for the case $\delta = \text{const}$, can be written as:

$$\frac{d\vartheta}{dt} + \frac{1}{cm} \left(\frac{kL}{S} - \delta^2 \rho_0 \alpha \right) \vartheta - \frac{kL}{cmS} \left(\frac{\delta^2 \rho_0 S}{kL} + \vartheta_0 \right) = 0. \quad (2.19)$$

By

$$\frac{kL}{S} > \delta^2 \rho_0 \alpha$$

Complete solution of the equation (2.19) is:

$$\vartheta(t) = C e^{\frac{1}{cm} \left(\frac{kL}{S} - \delta^2 \rho_0 \alpha \right) t} + \vartheta_y. \quad (2.20)$$

Assume that constant $C = \vartheta_n - \vartheta_y$. Then the solution of the equation (2.20) is:

$$\begin{aligned} \vartheta(t) &= \vartheta_y \left(1 - e^{\frac{1}{cm} \left(\frac{kL}{S} - \delta^2 \rho_0 \alpha \right) t} \right) + \vartheta_n e^{\frac{1}{cm} \left(\frac{kL}{S} - \delta^2 \rho_0 \alpha \right) t} = 90 \times \left(1 - e^{\frac{1,6}{0,05 \times 6,5} t} \right) + 23 \times e^{\frac{1,6}{0,05 \times 6,5} t} = \\ &= 90 - 67 \times e^{-4,92t}. \end{aligned}$$

Figure 2.4-a shows the temperature increase during the current heating process immediately after the current insertion moment. Characteristics of this function show, that temperature changes exponentially, aspired to setting value ϑ_y . Dependence of length changes

versus temperature changes $\Delta L=f(T)$ by constant load has been taken from the wire technical documentation [1] (fig.2.4.b)

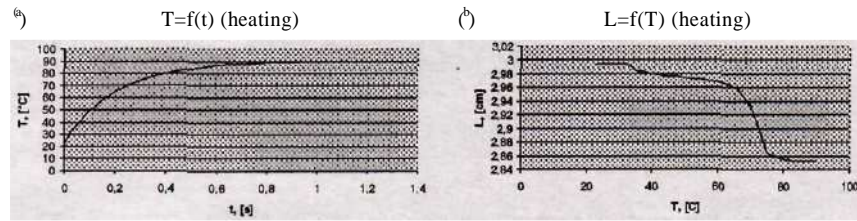


Fig.2.4. (a) The characteristic shows the temperature changes versus time during the heating process of Ni-Ti wire; (b) the characteristic shows the length changes versus temperature during the heating process of Ni-Ti wire

Then, from the dependence shown in figure 2.4.b, knowing T_1 in time Δt_1 , we can find the corresponding ΔL_1 , knowing T_1 in time Δt_2 we can find ΔL_1 . In addition, we became $L=f(t)$ (fig.2.5.a), where $t=\Delta t_1+\Delta t_2+\Delta t_3+\dots+\Delta t_n$.

In the figure 2.5.b the velocity function V versus time t has been depicted, which mathematical formula is found calculated from equations (2.7) and (2.11).

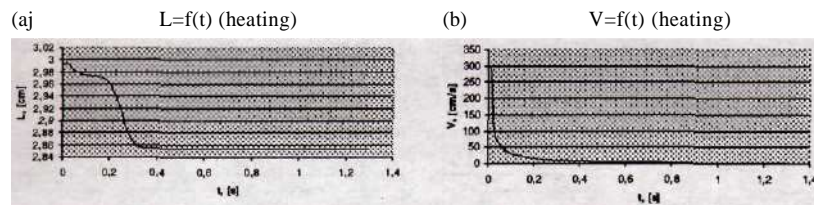


Fig.2.5. (a) The characteristic shows the length changes versus time during the heating process of Ni-Ti wire; (b) the characteristic shows the Ni-Ti wire contraction velocity changes versus time during the heating process

For Ni-Ti-wire cooling transformation processes calculation, in the case of the current starting point at the time moment $t=0$, we make following assumptions:

Then equation, describes the cooling process as:

$$\frac{d\vartheta}{dt} + \frac{kL}{cmS} \vartheta - \frac{kL}{cmS} \vartheta_0 = 0. \quad (2.21)$$

Its solution in the special case $\vartheta=\vartheta_n$ is:

$$\vartheta(t) = Ce^{-\frac{t}{\tau_0}} + \vartheta_0, \quad (2.22)$$

where

$$\tau_0 = \frac{cmS}{kL}.$$

The initial condition is $C = \vartheta_n - \vartheta_0$. Therefore, the complete solution of the equation (2.21) (fig.2.6) is

$$\vartheta(t) = (\vartheta_n - \vartheta_0)e^{-\frac{t}{\tau_0}} + \vartheta_0. \tag{2.23}$$

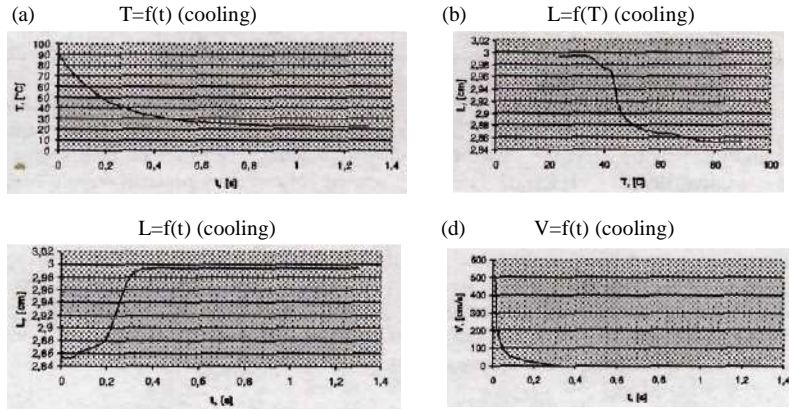


Fig.2.6. (a) The characteristic shows the temperature changes versus time during the cooling process of Ni-Ti wire; (b) the characteristic shows the length changes versus temperature during [he cooling process of Ni-Ti wire; (c) the characteristic shows the length changes versus time during the cooling process of Ni-Ti wire; (d) the characteristic shows the Ni-Ti wire contraction velocity changes versus time during the cooling process

3. BRAILLE DISPLAY CONTROL SYSTEM

In the third chapter we describe a Braille display control system. Braille display is a complex electro-mechanical device, controlled by a microcontroller and connected with a personal computer. One of its most important elements is the system of the mechanical graphical pattern recognition. This system provides the transfer of signals to the tactile sensor. This system allows the user to "scan" a text or a graphical pattern.

The motor's control node realises the functions of horizontal and vertical mechanical pattern resolution in the display for blind persons [10]. The very construction of the described node has been placed on one of the display's control plates.

The motor's control node receives digital codes of the rotation angle (phase) of the motor from a display's microcontroller. This node provides exact physical realisation of these angles and this way transfers the moves of the display module. The demands, enumerated in the first chapter, define a choice of a directly actuated collectorless constant current motor (DCCCM) as the base for the construction of a mechanical system for the pattern recognition in a display for blind persons. The stator's control turns commutation coils with respect to the position of the magnet poles of the rotor. The control achieved by a special scheme (driver), using signals of the rotor position sensors. The motor generates a variable magnet flux by its rotation. Under the influence of this flux on the Hall sensors, as an output, a sinusoidal signal is generated with the frequency proportional to the rotational velocity of the motor' roller. The formed signals from Hall sensors are used to cum on the stator's commutation.

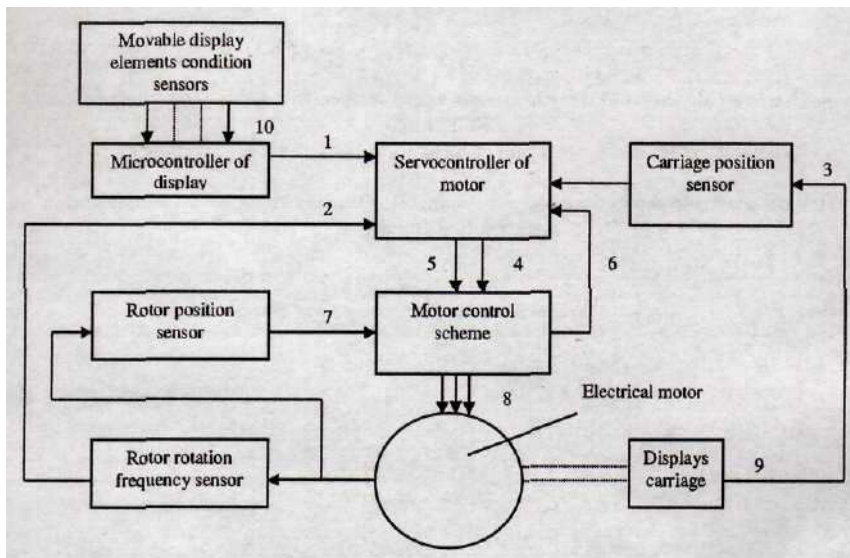


Fig.3.1. Scheme of the structure of the motor's control node

The motor's control node proposed for the display (fig.3.1) uses the automatically regulation system (ARS) [3] constructed on the principle of the two-channel (frequently-

phase) system with the closed back coupling in both channels [10]. The back coupling has been attained with the transference velocity sensor and the carriage position sensor.

The input influence on the control node is the digital code from the display's microcontroller [2]. The output value of the control node is the position of the carriage, on which the movable tactile module is situated.

The basic signals which define the functionality of the motor's control node (fig.3.1) are:

- 1 - digital code N_k of the setted carriage position, which is controlled in this channel, is a binary code of co-ordinate X (or Y for other channel) of the movable display module's position;
- 2 - signal MOTOR FG of the rotor rotation frequency sensor is a sinusoidal signal with short-dated (KpaTHOCTio) by frequency 40...60 to motor rotation frequency;
- 3 - signal N_f of the carriage's absolute position sensor is a digital two level code.
 - carrying information about the exact co-ordinate X (or Y for other channel) of the movable display module's position;
- 4 - output servocontroller signal N_j is the motor control signal MOTOR CTL;
- 5 - motor's reverse signal MOTOR REV;
- 6 - stator's current overloading signal CURRENT LIMIT;
- 7 - rotor's position sensor signal (forms the commutation signals PG);
- 8 - driver's output signal supplies the current for stator's turns DCCCM and defines motor's (rotor's) rotational velocity;
- 9 - signal PK of the relative position of the carriage sensor;
- 10 - signals of the movable display element's condition sensors provide display reliability and its defence from crushes.

To provide demanded accuracy (0,3%) of carriage with the tactile module position settings, the automatically regulation system has been used. It is constructed on the principle of two-channel (frequently-phase) system with the closed back coupling hi both channels and hi the non-linear node. It is used for the dynamical characteristic optimisation. The non-linear node is included in the algorithm for the calculation of the code N_d -

The aim of the non-linear node is to provide motor's rotational velocity optimisation by very large and very small disconcertions, therefore when the carriage is very far or very near to the setted position. This calculation, together with the code N_c calculation, form the so called discrimination characteristic. The velocity code N_c calculation is realised in the algorithm:

$$N_c = (X_f - X_k) \times K_o \times K_N. \quad (3.1)$$

The motor's control signal code N_d calculation plays a role of the two-channel discriminator. In the first channel of the discriminator is a sample signal, given by the value of N_c , compared to the exact value of the signal MOTOR FG frequency of the rotor's rotational frequency sensor (rough channel), and in the second channel the same sample signal is compared to the exact value of the signal PG of the rotor's position sensor frequency (exact channel).

The output signals of discriminator channels, added in the defined proportion (signal of exact channel has more weight), go to the pulse-width modulator as the code N_d . The pulse-width modulator has been applied in order to avoid the use of analogue elements in the servocontroller microscheme.

The output impulse sequence, equalised by a low pulse filter, as an analogue voltage MOTOR CTL goes to motor's control driver and gives the rotational velocity.

The functional scheme of such a system, which is functionally the motor's servocontroller, has been partly depicted on the figure 3.2.

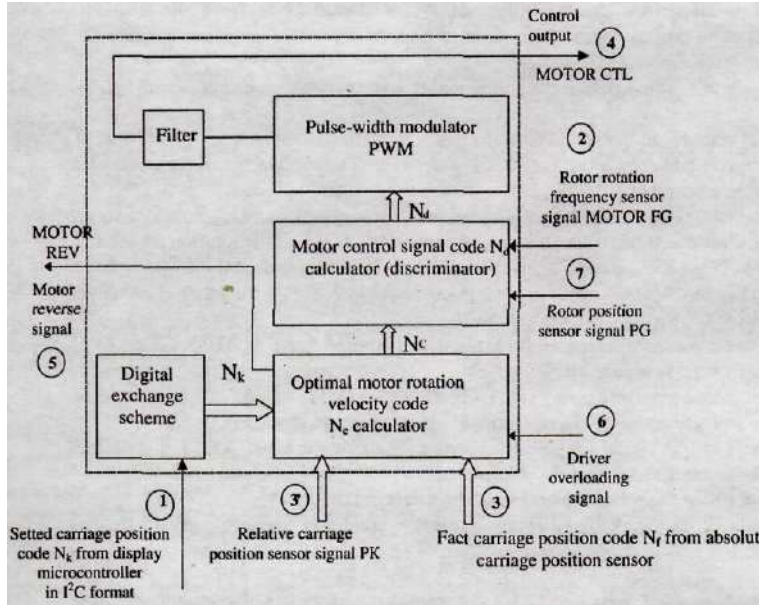


Fig.3.2. Functional scheme of the automatically regulation system

To analyse the dynamical characteristics, we make some assumptions:

- the servocontroller is a linear node in the automatically regulation system;
- we neglect the influence of the rough channel of the discriminator, which is made to provide the system stability in a case of outside brake of the carriage or sliding of the transmission between the motor and the carriage of the movable tactile module.

Taking into account that the velocity of the servocontroller's work is very high, and without any influences on transformation processes, we may assume it as a linear node. In compliance with functionality principle of the servocontroller-driver-motor node, which is a backward astatic regulation system, occurs an integration of disconcertion (difference between the setted and the actual (measured by the sensors) carriage position).

With these assumptions, the automatical regulation system obtains essential simplifications and includes only two dynamical nodes (fig.3.3).

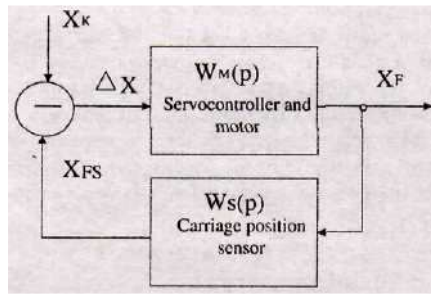


Fig.3.3. Structural scheme of the dynamical characteristics analysis

In this scheme with the servocontroller and the motor's amplify coefficient K , the following equations are valid:

$$W_M(p) = \frac{K_1}{p}, \quad (3.2)$$

$$\Delta X = X_k - X_{FS}, \quad (3.3)$$

$$W_M(p) = \frac{X_F}{\Delta X}, \quad (3.4)$$

$$W_S(p) = \frac{X_F}{X_k}. \quad (3.5)$$

If the carriage position sensor is a non-inertial node with $W_S(p) = 1$, then the transmission function of an open system is $W_E(p) = W_M(p)$, and the transmission function of a closed system [5] is:

$$W_z(p) = \frac{1}{T_1 p + 1}. \quad (3.6)$$

$$T_1 = (K_1)^{-1}. \quad (3.7)$$

The normalised transformation characteristic of a closed system in this case is described by the formula:

$$H(t) = 1 - e^{-\frac{t}{T_1}}. \quad (3.8)$$

Real sensors are represented as a node with the delay, or as an inertial node (aperiodical 1-st range). The transmission function $W_{S1}(p)$ is in the first case characterised with the equation:

$$W_{S1}(p) = e^{-pT_{s1}}, \quad (3.9)$$

or, in the second case ($W_{S2}(p)$) with:

$$W_{S2}(p) = \frac{1}{T_{s2} p + 1}. \quad (3.10)$$

If the carriage position sensor is a digital sensor (impulse counter) or a mechanical energy in a code transducer, then it represents a node with delay T_{sj} . In this case is physically a time period of the counter cycle (variant with counter) or a period of the transformation request (variant with direct transformation). If the position sensor is analogue (transformation of a mechanical value in voltage), then it represents an inertial node T_{sj} constant in time and given by a parameter of the equalised filter of the sensor. Taking into account (3.10), we obtain the transmission functions for an opened W_{gfp} and a closed $W_z(p)$ system:

$$W_{\varepsilon}(p) = \frac{K_1}{p(T_{s2}p + 1)} \quad (3.11)$$

and

$$W_z(p) = \frac{K_1(T_{s2}p + 1)}{p(T_{s2}p + 1) + K_1} \quad (3.12)$$

Using the obtained equations (3.11) and (3.12), we can evaluate the influence of the carriage position sensor inertia on the dynamical characteristics of the whole system. The best way to evaluate the influence of the sensor is to set the period of changes of a particular transformation process level. The character of the transformation process in the tactile module moving control system is defined by following equations:

$$p^2 + \frac{1}{T_{s2}}p + \frac{K_1}{T_{s2}} = 0 \quad (3.13)$$

and

$$p_{1,2} = -\frac{1}{2T_{s2}}(1 \pm (1 - 4T_{s2}K_1)^{0,5}). \quad (3.14)$$

The border, which divides the exponential and the vibrational character of the process is the condition:

$$T_{s2} = \frac{1}{4K_1} \quad (3.15)$$

With the condition

$$T_{s2} < \frac{1}{4K_1}, \quad (3.16)$$

decreases the setting time of the process. With the condition

$$T_{s2} > \frac{1}{4K_1} \quad (3.17)$$

occurs the overregulation and the setting time can increase compared to the case $T_{s2}=0$. If the executed condition is

$$T_{s2} = \frac{1}{4K_1}, \text{ then}$$

the transmission function of a closed system is:

$$W_z(p) = \frac{K_1(T_{s2}p + 1)}{T_{s2}(p + \frac{1}{2T_{s2}})^2} \quad (3.18)$$

The transformation characteristic of a closed system describes the equation:

$$H(t) = (1 - (1 + \frac{t}{4T_{s2}})e^{-\frac{t}{2T_{s2}}}) \quad (3.19)$$

If the condition

$$T_{s2} > \frac{1}{4K_1},$$

is fulfilled, then the transformation function of a closed system is defined by:

$$H(t) = 1 - e^{-(a_0 - a_1)t} + \frac{1}{b_1} ((a_0 - a_1)^2 + b_1^2)^{0,5} e^{-(a_0 - a_1)t} \sin(b_1 t), \quad (3.20)$$

$$a_1^2 + b_1^2 = \frac{K_1}{T_{s2}}, \quad a_0 = \frac{1}{T_{s2}}, \quad a_1 = \frac{1}{2T_{s2}}.$$

Calculation results $H(t)$ are partly depicted on the figure 3.4.

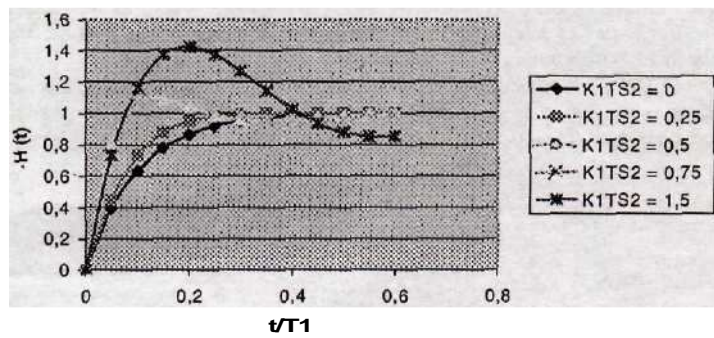


Fig.3.4. The character of the transformation characteristic $H(t)$ in depend of T/T_1 for different values of K_1 and T_s

For the position sensor with the transmission function $W_{s1}(p)$ (3.9), the transmission function of an opened and a closed systems is:

$$W_{\Sigma}(p) = \frac{K_1}{p} e^{(-pT_{s1})} \quad (3.21)$$

and

$$W_z(p) = \frac{K_1}{pe^{(-pT_{s1})} + K_1}. \quad (3.22)$$

After a decomposition of the value $e^{-pT_{s1}}$ we get:

$$e^{-pT_{s1}} = 1 - pT_{s1} + \frac{p^2 T_{s1}^2}{2!} - \frac{p^3 T_{s1}^3}{3!} + \dots \quad (3.23)$$

By limiting the series to the first three members, we obtain the equation of the transmission function of a dosed system:

$$W_z(p) = \frac{K_1}{p^2 T_{s1} + p + K_1} = \frac{K_1}{T_{s1}} \frac{1}{p^2 + \frac{p}{T_{s1}} + \frac{K_1}{T_{s1}}}. \quad (3.24)$$

Comparing the equations (3.12) and (3.24), we can see that the node with delay and the inertial node have an analogous character. The influences of the carriage position sensor of the tactile module with delay T_{sr} and of the inertial sensor T_{s2} of the dynamic of processes in the motor's control system of the display for blind persons, are similar as a result of a high velocity of the work. Taking into account that the display is a digital device with a microcontroller, to increase the regulation accuracy and to avoid the complementary analogue-digital reorganisations, a digital carriage position sensor has been chosen. The digital carriage position sensor is represented as a node with delay T_{si} from the position of view of the automatic regulation theory.

By analysis of dynamical characteristics of the control node we obtain:

- the character of the transformation process in the motor's control node is defined by the conformity of delay values in the carriage position sensor and the time constant of the motor's integration;
- the demands to calculator productivity, included into servocontroller, are formulated based on delay values in the carriage position sensor (the time period of the calculation cycle has to be 7-10 times smaller as the delay value T_{si}).

4. NATURAL TACTILE-GRAPHICAL MODULE SAMPLE AND LOGICAL ALGORITHMS OF ITS WORK

The fourth chapter describes a construction of the tactile-graphical Braille display. One of the elements, which define the practical value of this thesis is the developed electrical scheme of a display's prototype sample, and also a scheme-technical realisation of basic scheme nodes as a natural display's sample.

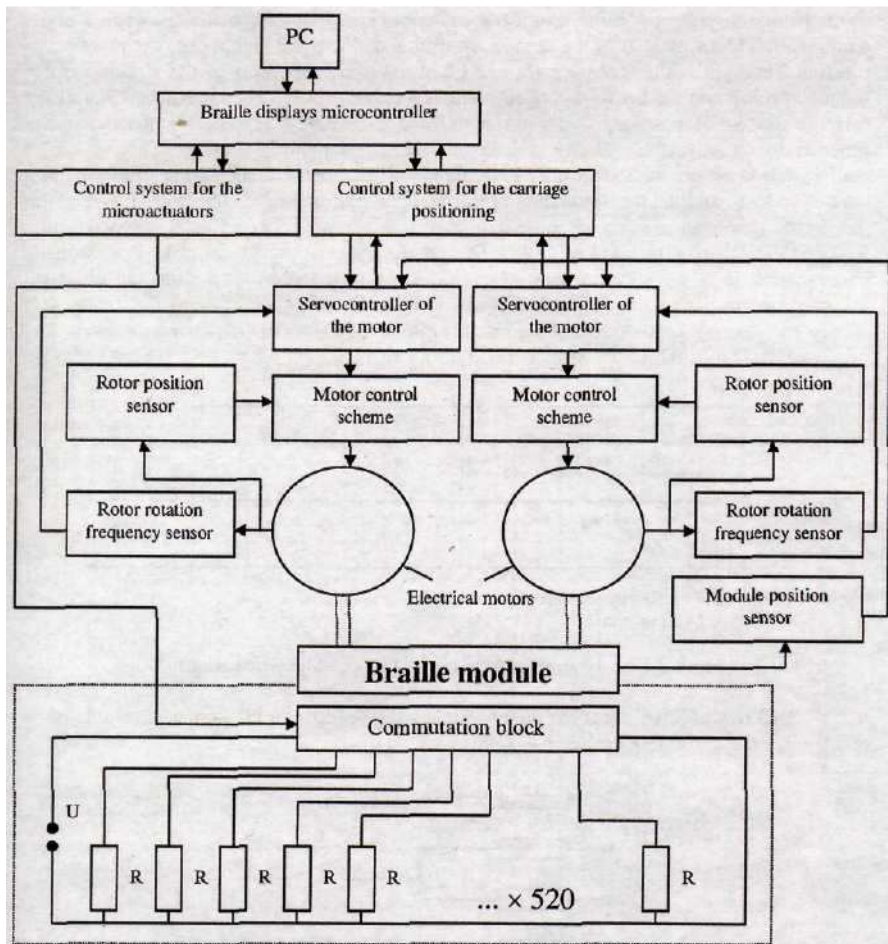


Fig.4.1. The general electrical scheme of the Braille display

On the generalised electrical scheme (fig.4.1) a movable module, with the size 40mm x 30mm, have been depicted. It includes $26 \times 20 = 520$ SMA microactuators R , which are supplied with the voltage U through the commutation block. The commutation block receives control signals from the control scheme. To each of the microactuators correspond some switches. They are situated in a serial microschemie - analogue switches are controlled by digital signals. The presented movable Braille module [7] transforms electronic pattern in a tactile - graphical information according to in the first chapter formulated demands.

A goal of the microactuator control node [2] is the transformation of pattern information codes. These codes come from a PC through the COM port in the microcontroller of the Braille display and further in the parallel control code of microactuator switches in the commutation block. A goal of the carriage control node [3] is the digital exchange scheme of the functional realisation (coming from a PC through the COM port in the Braille display microcontroller and further in described node, it receives from the codes N_{KV} and N^{\wedge} of the carriage the initial- position of the horizontal and the vertical graphical pattern) and the function to optimize the velocity code N_c calculator of motor's rotation. This system is realised based on the microcontroller PIC 16F84, which provides calculation of the motor's control code N_c and the transformation of this code in the format I²C. This format is used for the digital data transmission in the microschemie of a double two-channel servocontroller XRU/BU 2891 (manufactured by Sony). One of the important technical tasks is a current's commutation in SMA wires, which supply information transformation from the electrical presentation form into the mechanical form (relief). Switches $(S) \dots S_{mn}$ in the figure 4.2) supply the heating to the current's commutation of SMA wires in the matrix $m \times n$. The proposed cycle method for the SMA wires control (fig.4.2) is:

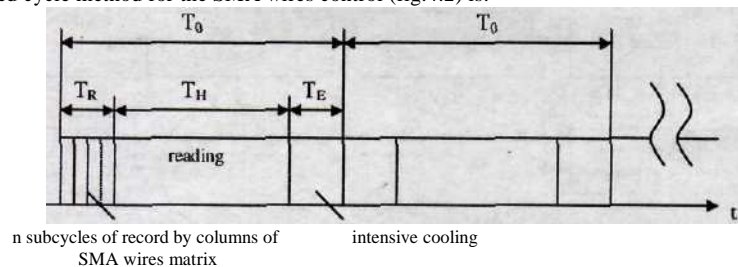


Fig.4.2. The diagram of time cycles by the SMA wires control

Each row of SMA wires has an individual source of current [9], and each column of SMA wires has one common switch (fig.4.3).

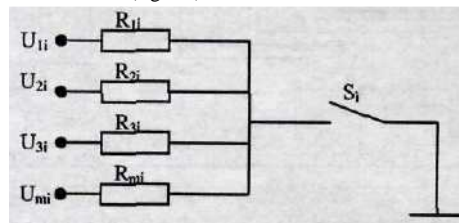


Fig.4.3. The electrical scheme of the SMA wires commutation block for the one column with the element quantity m

In the figure 4.3 $i = 1...n$. $R_{1i}...R_{mi}$ - are SMA wires (including complementary resistance) of i -th column. Altogether there are n columns. The common commutation block of the electrical scheme is presented in the figure 4.4. The main idea of commutation block's functionality is that, in the i -th element of a subcycle T_R , one end of the i -th column of each SMA wire is connected to the common wire through the switch S_i (of the set $DA1$). On the second end of the wire an information signal from outputs $DD3$ ("1" - heating occurs, "0" - no heating occurs) is submitted. The voltage of the information signal on the $DD3$ output is a source for this SMA wire.

Therefore, an impuls occurs heating the SMA wires through whole columns. The electrical connection of an SMA wire is as follows. The SMA wire has the contact points on its ends. One of them is electrically connected with the wire's columns. All of these wires are connected to the switches inputs DAL . The second end of the wire is electrically connected to the parallel wires.

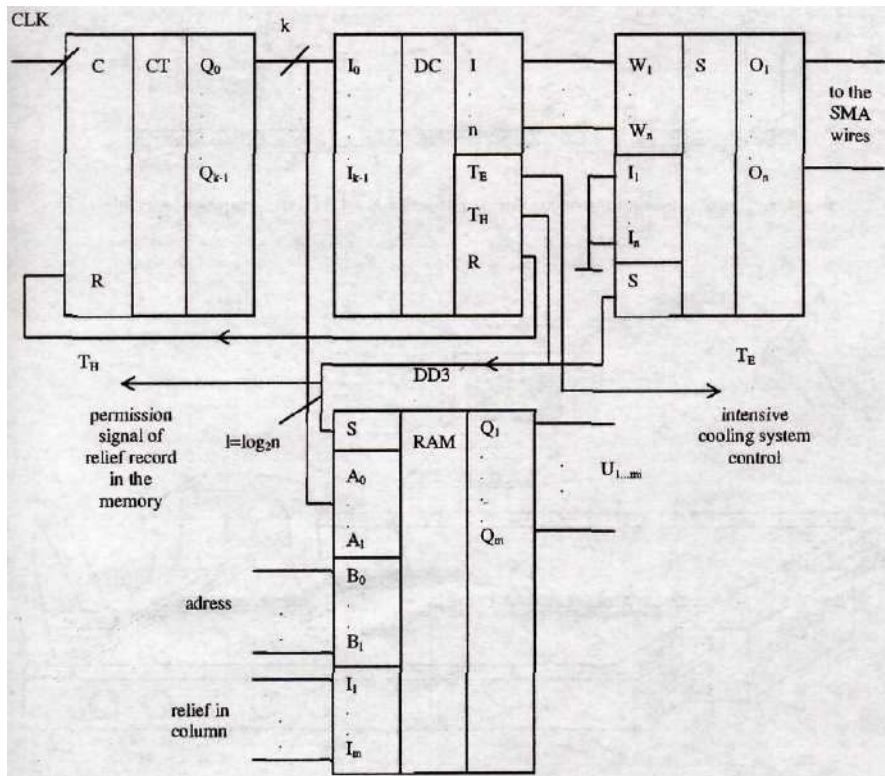


Fig.4.4. The general electrical scheme of the commutation block

A schematic microactuator construction of the movable tactile-graphical pattern module [12] is depicted in the figure 4.5. The microactuator consists of an SMA wire 3. One end of the wire is secured on the low plate 4. The second end of the SMA wire is mechanically clamped to the low end of the tactile-graphical pattern's taxel 1.

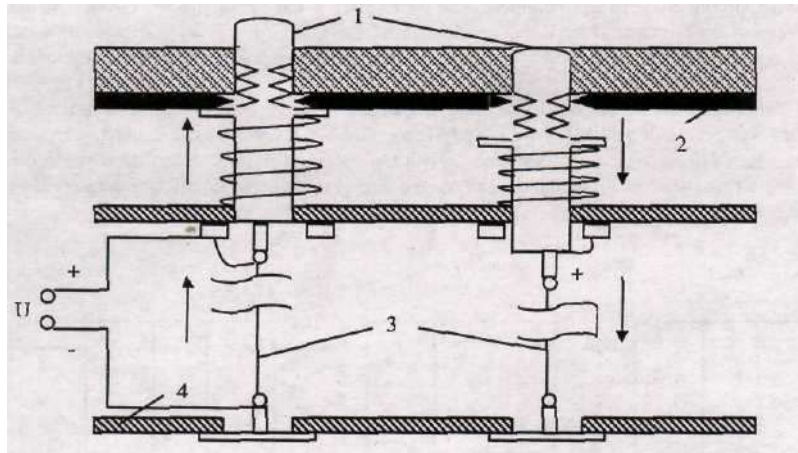


Fig.4.5. The schematic microactuator construction of the tactile-graphical module

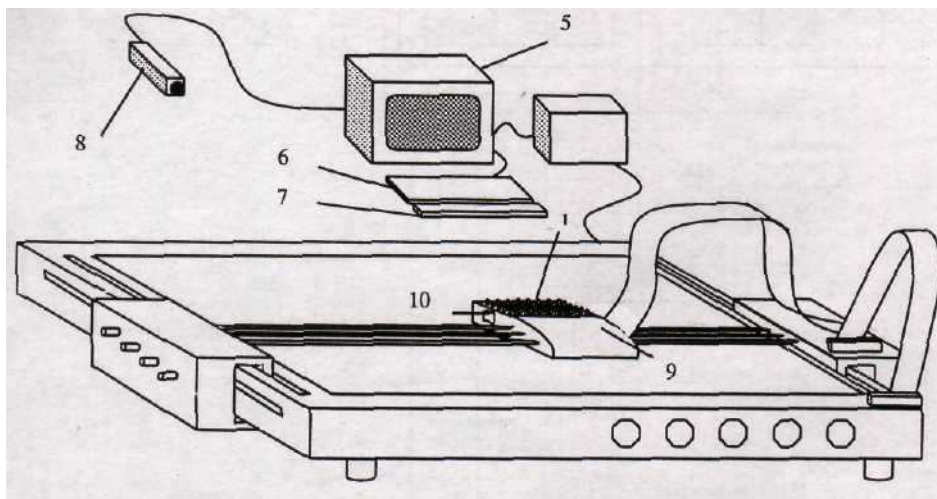


Fig.4.6. The schematic representation of the Braille display for blind persons with the movable tactile-graphical pattern module

With the current 70mA, the electrical power W_e on the taxel is calculated with the formula:

$$W_e = I^2 R_1 = 0,07^2 \times 14,16 = 0,07W. \quad (4.1)$$

If we take into account, that the module includes $n = 520$ pattern elements, and each of them needs a microactuator. the electrical power W needed for whole module can be calculated as:

$$W = \sum_{s=1}^{s=n} I^2 R_1 = \sum_{s=1}^{s=520} (0,07)^2 14,16 = 36W. \quad (4.2)$$

The Braille display (fig.4.6) [7, 12] has been supported with a personal computer 5 with a keyboard 6, and, what is particularly important for the blind persons, with a Braille script row 7. For the analysis of the Braille display as a whole, a video camera 8 may be used. The video camera is mounted to the module surface under such an angle, that all of the taxels and their positions are well recognisable. This information is sent to the computer, which, with the help of special algorithms, can quickly estimate the state of the Braille display and its readiness for the exploitation. The movable module 9 can be moved over the display surface by a user hand or controlled by the motor. The relief information, created by taxels, can be read out by sensing with user's fingers. During the movement of the movable module element, the state of the taxel changes according to module's position on the display's surface. The blocking plate 2 can be activated by a hand lever 10. All of the taxels can be blocked at the same time in their actual state with the parallel turn off of a voltage. In this way, it is possible to fix graphic pattern and use it for a long time without energy loses.

The request for such displays in Latvia can be estimated approximately to 7.000 - 35.000 units. Based on the analysis of one month work, the manufacturing costs of the five year production of the Braille display can be estimated. Taking one month production volumes: 117, 350 and 584 as the calculation basis, we become the manufacturing costs of one display in the range from 312,13 Ls (by 117 displays in month) till 309,13 Ls (by 584 displays in month). From the state of market of the tactile-graphical displays for blind persons we conclude, that the displays production must be oriented on export and can bring substantial economical results, because the production cost of a display is relative small and has no concurrence.

The algorithm for the pattern examination with the use of digital camera, is one of the new scientific results given in this chapter. This analysis is developed to examine the reliability of Braille display elements. The basis of the reliability conception is the variable of the crash possibility Q in a particular calendar period. Normally, one year will be taken as a calendar period. So we get:

$$Q = 1 - e^{-\lambda t}. \quad (4.3)$$

The calculations with this method are made by assumption that the time intervals between crashes obey the exponential distribution law. Therefore the following reliability variables can be used:

crash intensity for a display element

$$\lambda = \frac{1}{5 \times 365 \times 24 \times 520} = 4,3 \times 10^{-7}, \quad [1/h], \quad (4.4)$$

average working time till a crash occurs for a display element

$$T_{el} = \frac{1}{\lambda} = 2,2 \times 10^7, \quad [h], \quad (4.5)$$

average working time till a crash occurs for the whole module

$$T_m = \frac{1}{\lambda \times 520} = 4.4 \times 10^4, \text{ [h].}$$

(4.6)

Possibility of a crashless work of the device during 20 years

$$P(t) = e^{-\lambda t} = 0,976.$$

(4.7)

The reliability variables are based on the statistic. The statistic in this question is very limited, because this construction is new and there are very few similar devices on the market. That's why the intensity of crashes is based on experiments, which are made by the company manufacturing the Ni-Ti wires. Experiments show, that the wire is very reliable and holds hundreds of thousand cycles. After this number of cycles the wire stretches only by 0,5% from its initial length [1]. Therefore, we may assume that in one year work crashes one out of 520 taxels. To examine the Braille display work, the examination algorithms with the application of a video camera may be used (fig.4.7). The pattern from the camera is sent for the analysis to (he) computer.

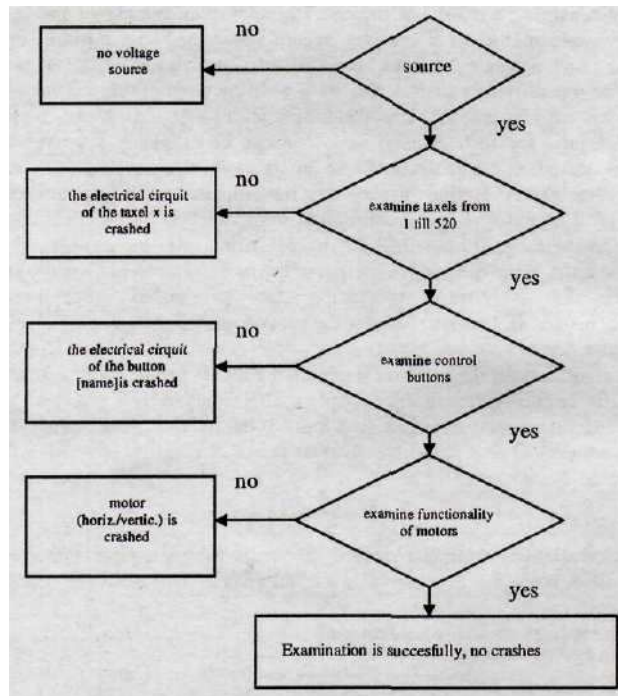


Fig.4.7. The examination algorithm of the Braille display before the work starts

A computer is modelling different patterns for a Braille display, which have to be realised on the surface. By the modelling, this process must be repeated with different velocities of the module. The pushing of control buttons is also simulated. If the crashes are detected, the programme informs about them and about their importance for the display's functionality.

An important complementary device, which makes the exploitation of a display easier, is a sound information transmitted by the computer to the speakers or to the ear-protectors. For example, the information about the crashes can be submitted this way. Typical phrases will be taken from the database with typical sentences for the possible situations.

In the fourth chapter some logical algorithms for the relief pattern creation have been also developed. They have, as a goal, the creation of the tactile-graphical patterns for blind persons in accordance to the module position on the display surface and in accordance to the control command_s received from the control buttons.

In this chapter we also analyse the utilisation of the display in accordance to the demands for the environment protection.

The tactile-graphical display for blind persons is able to work in three modes:

- user moves the module over the display surface by himself;
- the tactile-graphical pattern module is moved by the computer control by the motors;
- with the use of a keyboard and of a special program, a blind person can input in the computer the graphic pattern pushing on the keyboard buttons and simultaneously controlling it by the use of the Braille display.

GENERAL CONCLUSION

Dissertation results allow to resolve the qualitative tactile-graphical Braille display creation task on a new technical level:

1. The technical demands to tactile-graphical Braille display, based on psycho-physiological qualities of user analysis, are defined.
2. A patented method to form dynamical relief patterns in a tactile-graphical Braille display, based on SMA wires matrix, has been developed. The choice of the Ni-Ti-wire of length 30mm and diameter 50µm is established. It keeps loads till 250mN. The velocity of the reaction (<1s) allows to set quickly and reset a microactuator. The wire length changes in the range of 1mm as a result of the shape memory effect. Important advantages of this device are simplicity of construction and mounting, noiselessness and low costs.
3. The elongation-contraction process of SMA wire in display structure is theoretically and experimentally analyzed. The function $L=f(t)$ has been obtained from experimental results and with the use of the Lagrange polynomial have been calculated the function $V=f(t)$ - the dependence on taxel movement's velocity in time.
4. The thermal process of SMA wire in display structure is analyzed. The outgoing heat in SMA wire by a direct current heating is calculated. We have obtained the function of heating energy dependence in time $W=f(t)$, which includes a proportional and an exponential part. We have obtained the function of temperature dependence in time $T=f(t)$, which has an exponential character.
5. A structure of a movable tactile-graphical Braille display module and its control node structure have been developed. The structure includes the digital carriage position sensor, combined with the choice of collector-less motors DCCCM. This structure is a basis solution for the mechanical resolution system in the display. The algorithms for the motor's control signal calculation, based on two-channel ARS, have been proposed.
6. Dynamical properties of display's motor control system have been analyzed. For display's control system development we used a mathematical modeling. The analysis of the control node dynamical characteristics shows that the character of the transition processes in the motor's control node is defined by the correlation between the backward value in the carriage position sensor and the constant of the motor integration time.
7. A method of the relief pattern generation, based on cycle approach to SMA wires control, have been proposed.
8. We have created and tested a sample of a movable Braille display tactile module, which is able to quickly, cheaply and safely transmit a tactile information. The novelty of the construction is that Braille pattern presentation occurs on a relative small movable module, and not on the large area, what decreases the device costs. To increase the safety of the device we have developed a test system based on logical algorithms. These algorithms include: test of energy source, taxel and keys system test and test of motor's circuits. In the interactive work mode, the user is able to create a tactile pattern by himself with a keyboard of PC and to examine this pattern on the surface of the Braille display.
9. We have calculated the consumption of energy of the movable module to 36W. The costs of Braille display manufacturing have been analyzed and they are 309Ls - 312Ls.

- ■

REFERENCES

1. Dynalloy, Inc. Technical characteristics of Flexinol actuator wires, 2002, pp. 1-12.
2. Greivulis J., Raņķis J.: Jekārtu vadības elektroniskie elementi un mezgli, Rīga, Avots, 1997, Ipp. 288.
3. Osis J.: Automātiskā vadība un regulēšana, Rīga. Zvaigzne, 1969, Ipp. 268.
4. Seelecke S., "Adaptive Suiiktoren mit SMA-Aktoren - Modellierung und Simulation", Habilitationsschrift. Berlin, 1999 s. 6-15.
5. Бесекерский В. А. Теория регулирования автоматич. систем. -М.: Знание. 1975, с. 520.
6. Залесский А.М., Кукеков Г.А.: Тепловые расчёты -электрических аппаратов, издательство Энергия, Ленинградское отделение, 1967. с. 10-11.

AUTOR PUBLICATIONS

7. Graf R. Experimental Research: Shape Memory Alloys - Actuator for Using in Movable Graphical Device for Visually Impaired People, Mikroelektronik 2003, tictober 1-2, 2003, Vienna, Austria.
8. Ouchkalov R., Brenner W., Mitic S., Popovic G., Vujanic A. Micro Actuation Principles for Tactile Graphic Displays (state of the art and recent efforts). Proc of ihe MME'99, september 27-28,1999, Gif sur Yvette, France, pp. 247-250.
9. Ouchkalov R., Brenner W., Mitic S., Popovic G., Vujanic A., Medek R. Development of microactuators for tactile graphic displays (state of the art and recent efforts). Proc of the 22nd International Conference on Microelectronics (MIEL 2000), Vol 2, may 14-17, 2000. Niš, Serbia, pp. 573-576.
10. Uškalovs R. Greivulis J. Braila displeja dzinēja vadības sistēmas dinamisko raksturlīknu analīze, "Enerģētika un elektrotehnika" RTU zinātniskie raksti, sērija 4, sējums 7, Rīga 2002, izdevniecība RTU. Ipp. 105-1,10.
11. Uškalovs R. Greivulis J. Šķidrumu ar īpašajām elektriskajām struktūrām pielietojums Braila displeja izveidē, "Enerģētika un elektrotehnika" RTU zinātniskie raksti, sērija 4, sējums 5, Rīga 2002, izdevniecība RTU,)pp. 110-113.

PATENT OF INVENTION

12. Graf R., Austrian patent: A 259/2003, "Kompaktes Bewegliches Taktiles Modul Mit Formgedächtnislegierungen-Antrieb", 20.02.2003.

